

## On the Mechanism of the Acid/Base-Catalyzed Thermal *Cis–Trans* Isomerization of Methyl Orange

Ana M. Sanchez,<sup>†,‡</sup> Mónica Barra,<sup>\*,†</sup> and Rita H. de Rossi<sup>\*,§</sup>

Department of Chemistry, University of Waterloo, Waterloo, Ontario, Canada, N2L 3G1, and Instituto de Investigaciones en Físico-Química de Córdoba (INFIQC), Facultad de Ciencias Químicas, Departamento de Química Orgánica, Universidad Nacional de Córdoba, 5000, Córdoba, República Argentina

Received October 14, 1998

The thermal *cis–trans* isomerization of methyl orange (i.e., sodium 4-[4'-(dimethylamino)phenylazo]-benzenesulfonate) in acidic aqueous solutions has been investigated by means of laser-flash photolysis techniques. The thermal *cis–trans* isomerization is found to be catalyzed by general acids and general bases. Catalysis is attributed to acid/base-assisted tautomerization of *cis*-ammonium ions (formed by rapid protonation of *cis*-methyl orange generated upon photochemically induced *trans–cis* isomerization) into *cis*-azonium ions. The latter can easily isomerize via rotation around the  $-N=N-$  bond as a result of the concomitant decrease in the double bond character. Furthermore, the acidity of *cis*-ammonium ions is estimated to be significantly lower than that reported for the *trans* isomers ( $pK_a$  values are 5.0 and 2.70–2.87, respectively). This result is attributed to a decrease in resonance interactions of the two aryl rings in the *cis* isomer compared with the *trans* form due to the nonplanar conformation of the former.

### Introduction

Over the last 50 years, numerous groups have investigated various aspects of the photoinduced and thermally induced *cis–trans* isomerization mechanism of azobenzenes. The reversible isomerization of azobenzenes is subject of current interest due to potential application of azobenzenes as photoactive compounds for molecular devices such as information storage systems and photochemical switching systems.<sup>1</sup>

Mechanistic studies of the thermal *cis–trans* isomerization of azobenzenes have focused on the effects of substituents,<sup>2–5</sup> solvent polarity,<sup>2–4,6,7</sup> and pressure<sup>8–10</sup> on the rate of this reaction. Two different mechanisms have been proposed for this process: *cis–trans* isomerization may proceed (i) via *rotation* about the  $-N=N-$  bond,<sup>2,11–13</sup> or (ii) via *inversion* of one of the nitrogen atoms (by means of an *sp*-hybridized transition state).<sup>3–6,8–10,13,14</sup>

Although the thermal *cis–trans* isomerization of azobenzenes is known to be catalyzed by Brønsted and Lewis acids, very little work has been conducted in this area.<sup>15–17</sup> In recent reports, it has been shown that the rate of the thermal *cis–trans* isomerization of 4-(dimethylamino)-azobenzene derivatives is strongly inhibited by hydroxide ions.<sup>18,19</sup> Protonated 4-(dimethylamino)azobenzenes are shown to isomerize at least  $10^8$  times faster than the corresponding conjugate forms. Monoprotonated azo compounds possessing *p*-amino groups exist indeed as equilibrium mixtures of two tautomers, i.e., the ammonium and the azonium ions (eq 1). The latter are believed to be able to easily isomerize via *rotation* about the  $-N=N-$  bond due to a decrease in the double bond character. Thus, inhibition by hydroxide ions would arise from the resulting decrease in the concentration of the more reactive azonium ions.

To gain further insights into the acid-catalyzed isomerization mechanism of 4-(dimethylamino)azobenzenes, time-resolved laser flash photolysis techniques were applied to the study of the thermal *cis–trans* isomerization of methyl orange (**MO**,  $R = SO_3^- Na^+$ ) as a model compound, in buffered aqueous solutions at  $pH < 7.0$ . The results of such a study are presented here.

### Results

Laser excitation, at 355 nm, of buffered aqueous solutions of **MO** ( $7 > pH > 5.5–5.0$ ) results in photochemically induced *trans–cis* isomerization. Due to the fact that extinction coefficients for *cis* isomers in the visible region are lower than the corresponding ones for

<sup>†</sup> University of Waterloo.

<sup>‡</sup> Present address: Sealy Center for Molecular Science, University of Texas Medical Branch, Galveston, TX 77555-1071.

<sup>§</sup> Universidad Nacional de Córdoba.

(1) (a) Bach, H.; Anderle, K.; Fuhrmann, Th.; Wendorff, J. H. *J. Phys. Chem.* **1996**, *100*, 4135. (b) Enomoto, T.; Hagiwara, H.; Tryk, D. A.; Liu, Z.-F.; Hashimoto, K.; Fujishima, A. *J. Phys. Chem.* **1997**, *101*, 7422, and references therein.

(2) Wildes, P. D.; Pacifici, J. G.; Irick, G., Jr.; Whitten, D. G. *J. Am. Chem. Soc.* **1971**, *93*, 2004.

(3) Nishimura, N.; Sueyoshi, T.; Yamanaka, H.; Imai, Y.; Yamamoto, S.; Hasegawa, S. *Bull. Chem. Soc. Jpn.* **1976**, *49*, 1381.

(4) Marcandalli, B.; Liddo, L. P.; Fede, C. D.; Bellobono, I. R. *J. Chem. Soc., Perkin Trans. 2* **1984**, 589.

(5) Brown, E. V.; Granneman, G. R. *J. Am. Chem. Soc.* **1975**, *97*, 621.

(6) Haberfeld, P.; Block, P. M.; Lux, M. S. *J. Am. Chem. Soc.* **1975**, *97*, 5804.

(7) Schanze, K. S.; Mattox, T. F.; Whitten, D. G. *J. Org. Chem.* **1983**, *48*, 2808.

(8) Asano, T.; Okada, T.; Shinkai, S.; Shigematsu, S.; Kusano, Y.; Manabe, O. *J. Am. Chem. Soc.* **1981**, *103*, 5161.

(9) Asano, T.; Yano, T.; Okada, T. *J. Am. Chem. Soc.* **1982**, *104*, 4900.

(10) Nishimura, N.; Tanaka, T.; Asano, M.; Sueishi, Y. *J. Chem. Soc., Perkin Trans. 2* **1986**, 1839.

(11) LeFevre, R. J. W.; Northcott, J. *J. Chem. Soc.* **1953**, 867.

(12) Schulte-Frodlinde, D. *Liebigs Ann. Chem.* **1958**, *612*, 138.

(13) Asano, T.; Okada, T. *J. Org. Chem.* **1986**, *51*, 4454.

(14) Otruba, J. P. I.; Weiss, R. G. *J. Org. Chem.* **1983**, *48*, 3448.

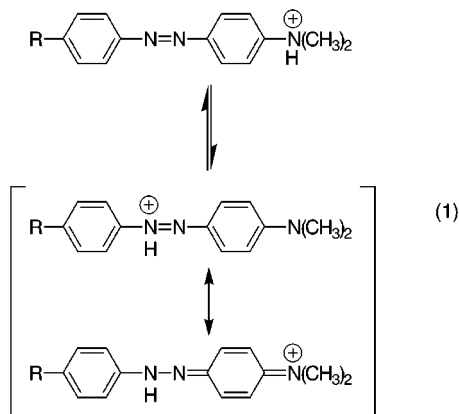
(15) Ciccone, S.; Halpern, J. *Can. J. Chem.* **1959**, *37*, 1903.

(16) Lovrien, R.; Waddington, J. C. B. *J. Am. Chem. Soc.* **1964**, *86*, 2315.

(17) Wettermark, G.; Langmuir, M. E.; Anderson, D. G. *J. Am. Chem. Soc.* **1965**, *87*, 476.

(18) Sanchez, A. M.; de Rossi, R. H. *J. Org. Chem.* **1993**, *58*, 2094.

(19) Sanchez, A. M.; de Rossi, R. H. *J. Org. Chem.* **1995**, *60*, 2974.



trans isomers,<sup>2,20</sup> instantaneous bleaching is observed (Figure 1). As the thermal *cis-trans* isomerization proceeds, complete recovery of the initial absorbance of the solution is observed, indicating that the entire process is reversible. Furthermore, transient absorption spectra obtained under these experimental conditions are essentially mirror images of the corresponding ground-state absorption spectra of the solutions.

Recovery traces follow first-order kinetics (Figure 1, inset), and deaerating the solutions shows no measurable effect. The resulting observed rate constants ( $k_{\text{obs}}$ , Tables S1–S3), independent of monitoring wavelength, are highly dependent on proton concentration as well as on buffer concentration. Plots of  $k_{\text{obs}}$  vs total buffer concentration ( $[\text{buffer}]_{\text{T}}$ ) are nonlinear and approach asymptotically a plateau region (Figure 2 is representative), a result which could be attributed to a change in rate-controlling step. Moreover, plots of  $1/k_{\text{obs}}$  vs  $1/[\text{buffer}]_{\text{T}}$  are satisfactorily linear (Figure 3), which suggest that  $k_{\text{obs}}$  values may be related to  $[\text{buffer}]_{\text{T}}$  according to eq 2, where  $P(1)$  and  $P(2)$  represent kinetic parameters.

$$k_{\text{obs}} = \{P(1)[\text{buffer}]_{\text{T}} / (1 + P(2)[\text{buffer}]_{\text{T}})\} \quad (2)$$

Nonlinear fittings of  $k_{\text{obs}}$  values according to eq 2 lead to the adjustable kinetic parameters  $P(1)$  and  $P(2)$  shown in Table 1.<sup>21</sup> Clearly, the resulting values depend on the type of buffer as well as on pH. While a nonlinear fitting was preferred, it is important to point out that the kinetic parameters obtained from the slope and intercept corresponding to plots of  $1/k_{\text{obs}}$  vs  $1/[\text{buffer}]_{\text{T}}$  are in excellent agreement with the values shown in Table 1.

When working at lower pHs (i.e., pH < 5.5, succinate buffer; pH < 5.0, acetate buffer), in addition to bleaching a weak transient absorption band in the 500–600 nm region is observed (Figure 4). As in the case of the series at pH > 5.0, the entire process is reversible, and deaerating the solutions shows no measurable effect. Spectra of the type shown in Figure 4 clearly indicate the presence of more than one absorbing transient species. It is well-known that the UV–visible spectra of monoprotonated 4-aminoazobenzene derivatives display two strong peaks, the band at longer wavelengths (typically in the 500–540 nm region) being attributed to azonium ions.<sup>22</sup> Thus, the transient absorption band

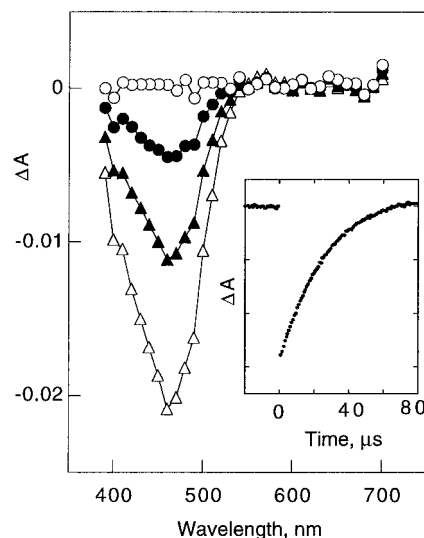


**Figure 1.** Transient absorption spectra for MO (pH = 7.00, phosphate buffer) obtained within 2  $\mu\text{s}$  ( $\Delta$ ) and 250  $\mu\text{s}$  ( $\circ$ ) after laser pulse. Inset: kinetic trace recorded at 430 nm.

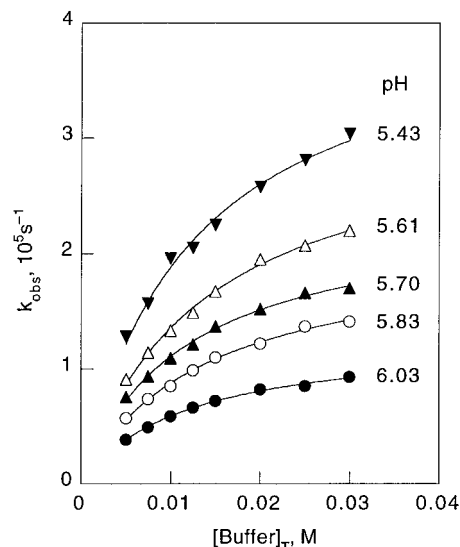


**Figure 2.** Buffer concentration dependence of the observed rate constant for *cis-trans* isomerization of MO in buffered aqueous solution (succinate buffer).

observed when working at low pHs is tentatively attributed to *cis*-azonium ions (see below).

As it can be inferred from Figure 4, kinetic traces vary with monitoring wavelength ( $\lambda_{\text{monitoring}}$ ). At wavelengths shorter than 450 nm, however, kinetic traces are independent of  $\lambda_{\text{monitoring}}$ . Traces recorded at 430 nm follow first-order kinetics up to at least three lifetimes, and resulting  $k_{\text{obs}}$  values (Tables S2 and S3) show a nonlinear dependence on  $[\text{buffer}]_{\text{T}}$  (plots not shown), as observed when working at pH > 5.0. At  $\lambda_{\text{monitoring}} > 500$  nm, a growth signal followed by a decay are detected (Figure 4, inset). The rates for these two processes are quite close; therefore, a precise evaluation of the corresponding rate constants becomes difficult. However, when kinetic traces of the type shown in Figure 4 (inset) are fitted to a double exponential function, the smallest rate constant (i.e., decay process) agrees fairly well with the value determined from the recovery signal collected at 430 nm. Thus, rate constants determined at 430 nm were employed to extract, from the kinetic traces recorded at 540 nm,  $\Delta A$ ,

(20) Brode, W. R.; Gould, J. H.; Wyman, G. M. *J. Am. Chem. Soc.* **1952**, *74*, 4641.

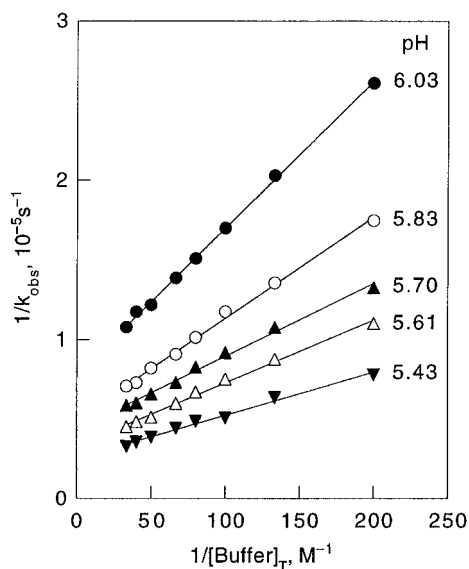
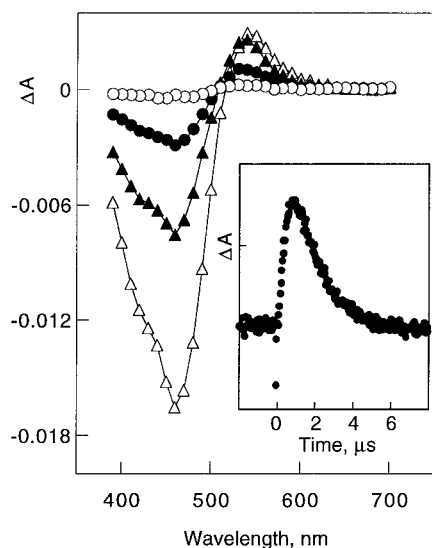
(21) Fittings were carried out by using the general curve fitting procedure of Kaleidagraph 3.0.5 software from Synergy Software.

(22) Lewis, G. E. *Tetrahedron* **1960**, *10*, 129.

**Table 1. Kinetic Parameters for the Thermal *Cis-Trans* Isomerization of MO in Buffered Aqueous Solution<sup>a</sup>**

$x_i^b$	phosphate buffer		$x_i^b$	succinate buffer		$x_i^b$	acetate buffer	
	$P(1)$ $10^6 \text{ M}^{-1} \text{ s}^{-1}$	$P(2)$ $\text{M}^{-1}$		$P(1)$ $10^7 \text{ M}^{-1} \text{ s}^{-1}$	$P(2)$ $\text{M}^{-1}$		$P(1)$ $10^7 \text{ M}^{-1} \text{ s}^{-1}$	$P(2)$ $\text{M}^{-1}$
0.437	$4.2 \pm 0.2$	$185 \pm 9$	0.129	$1.09 \pm 0.03$	$85 \pm 4$	0.078	$1.34 \pm 0.04$	$49 \pm 3$
0.563	$5.6 \pm 0.3$	$158 \pm 13$	0.189	$1.52 \pm 0.05$	$73 \pm 4$	0.114	$2.01 \pm 0.09$	$47 \pm 4$
0.651	$6.4 \pm 0.4$	$117 \pm 12$	0.239	$2.08 \pm 0.08$	$87 \pm 5$	0.170	$3.0 \pm 0.1$	$50 \pm 4$
0.734	$7.8 \pm 0.4$	$110 \pm 8$	0.278	$2.35 \pm 0.09$	$74 \pm 5$	0.258	$4.6 \pm 0.2$	$56 \pm 6$
0.784	$8.6 \pm 0.5$	$93 \pm 9$	0.366	$3.4 \pm 0.2$	$81 \pm 7$			

<sup>a</sup> At 21 °C,  $I = 0.2 \text{ M}$  (NaCl). <sup>b</sup> Molar fraction of acidic component of buffer.

**Figure 3.** Plot of  $1/k_{\text{obs}}$  vs  $1/[\text{buffer}]_{\text{T}}$  for MO in buffered aqueous solutions (acetate buffer).**Figure 4.** Transient absorption spectra for MO (pH = 4.5, acetate buffer) obtained within  $0.7 \mu\text{s}$  ( $\Delta$ ) and  $7.0 \mu\text{s}$  ( $\circ$ ) after laser pulse. Inset: kinetic trace recorded at 540 nm.

values (where  $t$  refers to time) corresponding to the fastest process. Resulting traces followed first-order kinetics up to at least two lifetimes, and the corresponding rate constants values ( $k_{\text{growth}}$ ) are summarized in Table 2. We tentatively attribute this process to the formation of *cis*-ammonium and *cis*-azonium ions by fast protonation of the amino and azo groups of the substrate. At these low pHs, the high hydronium ion concentration leads to accumulation of the protonated species, and the

**Table 2. Growth Rate Constant ( $k_{\text{growth}}$ ) for *Cis-Trans* Isomerization of MO in Buffered Aqueous Solution as a Function of Total Buffer Concentration and pH<sup>a</sup>**

[buffer] <sub>T</sub> , M	$k_{\text{growth}}, 10^6 \text{ s}^{-1} \text{ }^b$		
	4.73 <sup>c</sup>	4.55 <sup>c</sup>	4.60 <sup>d</sup>
0.0050	1.50	1.72	1.82
0.0075	1.90	1.96	2.11
0.010	2.10	2.44	2.30
0.0125	2.50	2.62	2.65
0.015	2.60	2.65	2.92
0.020	3.10	3.20	3.22
0.025	3.60	3.59	3.51
0.030	3.75	4.00	4.00

<sup>a</sup> At 21 °C,  $I = 0.2 \text{ M}$  (NaCl),  $\lambda_{\text{monitoring}} = 540 \text{ nm}$ . <sup>b</sup> Error  $\pm 15\%$ . <sup>c</sup> Acetate buffer. <sup>d</sup> Succinate buffer.

system then relaxes in a slower process to the thermodynamic equilibrium. The values of the observed rate constant for the fast process ( $k_{\text{growth}}$ ) are given by eq 3,

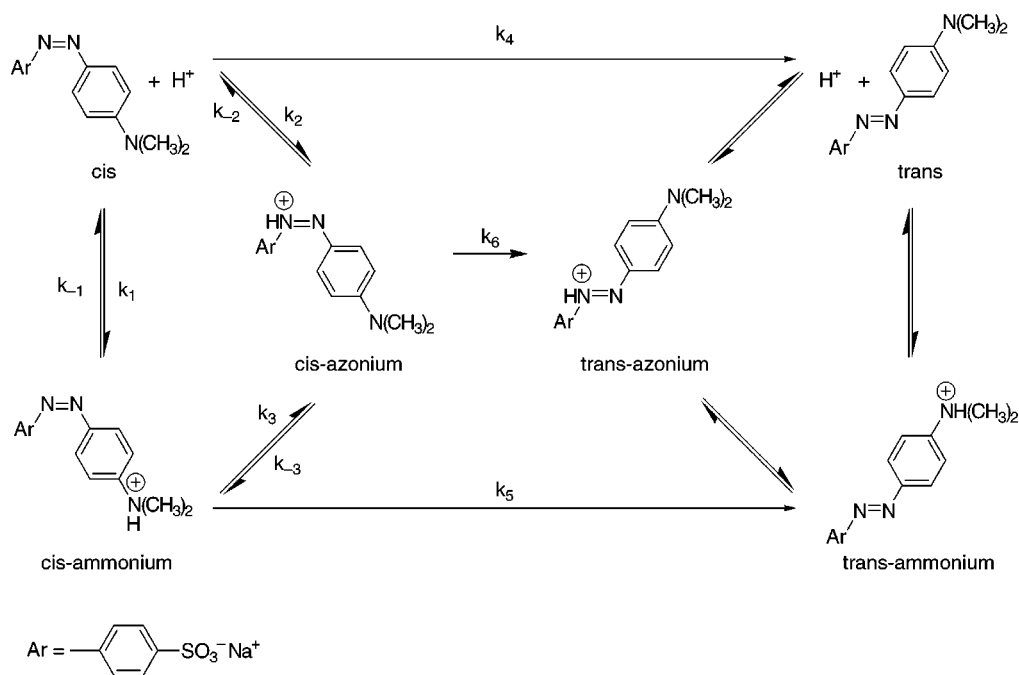
$$k_{\text{growth}} = (k_1^{\text{H}^+} + k_2^{\text{H}^+})[\text{H}^+] + (k_1^{\text{acid}} + k_2^{\text{acid}})x_i[\text{buffer}]_{\text{T}} \quad (3)$$

where  $k_1$  and  $k_2$  refer to Scheme 1, and  $x_i$  represents the molar fraction of acidic component of the buffer. Plots of  $k_{\text{growth}}$  vs  $(x_i[\text{buffer}]_{\text{T}})$  are satisfactorily linear (plots not shown), in agreement with eq 3. The ratio between the intercept value and the corresponding hydronium ion concentration yields (at pH 4.73, 4.55, and 4.60, respectively)  $4.9 \times 10^{10}$ ,  $3.7 \times 10^{10}$ , and  $4.5 \times 10^{10} \text{ M}^{-1} \text{ s}^{-1}$ , consistent with diffusion-controlled protonation rate constants.<sup>23</sup> Also, the slope values for the acetate-catalyzed series are in good agreement with each other, namely,  $1.83 \times 10^8$  and  $1.48 \times 10^8 \text{ M}^{-1} \text{ s}^{-1}$ , whereas for the succinate buffer series, the resulting value is  $1.22 \times 10^8 \text{ M}^{-1} \text{ s}^{-1}$ . However, due to the limited number of data that could be obtained at low pHs, as a result of the low solubility of MO under these experimental conditions, we will not discuss these results any further.

## Discussion

The thermal *cis-trans* isomerization of MO is proposed to be represented as shown in Scheme 1. According to Scheme 1, *cis*-azonium ions (transient species absorbing at  $\lambda > 500 \text{ nm}$ ) are generated by (i) acid/base-catalyzed tautomerization of *cis*-ammonium ions (assumed to be formed by rapid protonation of *cis*-MO generated upon 355-nm laser induced *trans-cis* isomerization), and (ii) acid-catalyzed protonation of *cis*-MO. On the basis of the inhibition of MO isomerization by HO<sup>-</sup> previously reported,<sup>18,19</sup> and the fact that the observed rate constant does not show any buffer independent term (see below),

Scheme 1



we conclude that  $k_4$  and  $k_5$  are negligible. In addition, the *cis-trans* isomerization of 1-hydroxy-4-(phenylazo)-naphthalene is shown to be extremely fast as a result of isomerization proceeding via the hydrazone isomer.<sup>24</sup> Thus, only  $k_6$  becomes significant in the present case.

Assuming that, for the data taken at pH > 5.0, *cis*-azonium ions are steady-state intermediates, the expression for the corresponding observed rate constant would be given by eq 4

$$k_{\text{obs}} = k_0 + \frac{k_6 \{ (f[k_3^{\text{acid}} x_1 + k_3^{\text{base}} (1 - x_1)] + (1 - f)k_2^{\text{acid}} x_1 \} [\text{buffer}]_{\text{T}}}{k_6 + \{ k_{-3}^{\text{acid}} x_1 + (k_{-3}^{\text{base}} + k_{-2}^{\text{base}})(1 - x_1) \} [\text{buffer}]_{\text{T}}} \quad (4)$$

where  $f = \{ [H^+] / ([H^+] + (k_{-1}/k_1)) \}$ ,  $x_1$  represents the molar fraction of acidic component of the buffer,  $k^{\text{acid}}$  and  $k^{\text{base}}$  represent catalytic rate constants for the acidic and basic components of the buffer, and  $k_0$  represents the buffer independent rate constant.<sup>25</sup> As already mentioned, plots of  $1/k_{\text{obs}}$  vs  $1/[\text{buffer}]_{\text{T}}$  at pH > 5.0 are linear (Figure 3), which indicates that under these experimental conditions, the buffer independent term ( $k_0$ ) is indeed negligible. Thus, the comparison of eq 4 with eq 2 results in the kinetic parameters  $P(1)$  and  $P(2)$  given by eq 5 and 6.

$$P(1) = (f) \{ k_3^{\text{acid}} x_1 + k_3^{\text{base}} (1 - x_1) \} + (1 - f) k_2^{\text{acid}} x_1 \quad (5)$$

$$P(2) = \{ k_{-3}^{\text{acid}} x_1 + (k_{-3}^{\text{base}} + k_{-2}^{\text{base}})(1 - x_1) \} / k_6 \quad (6)$$

(24) Fischer, E.; Frei, Y. F. *J. Chem. Soc.* **1959**, 3159.

(25) From the steady-state approximation for *cis*-azonium ions,  $k_0$  is given by

$$k_0 = \frac{k_6 \{ (f) \{ k_3 + k_3^{\text{H}^+} [H^+] + k_3^{\text{OH}^-} [\text{OH}^-] \} + (1 - f) (k_2 + k_2^{\text{H}^+} [H^+]) \}}{k_6 + \{ k_{-3} + k_{-3}^{\text{H}^+} [H^+] + k_{-2} + (k_{-3}^{\text{OH}^-} + k_{-2}^{\text{OH}^-}) [\text{OH}^-] \}}$$

To evaluate the catalytic rate constants involved in eq 5, it becomes necessary to determine the value of  $f = \{ [H^+] / ([H^+] + (k_{-1}/k_1)) \}$ . This, in turn, requires the value of the acid dissociation equilibrium constant of *cis*-ammonium ions (i.e.,  $K_a = k_{-1}/k_1$ ). Rearrangement of eq 4 ( $k_0$  negligible) leads to eq 7,

$$\frac{1}{k_{\text{obs}}} = \frac{1 + \{ [k_{-3}^{\text{acid}} x_1 + (k_{-3}^{\text{base}} + k_{-2}^{\text{base}})(1 - x_1) \} / k_6 [\text{buffer}]_{\text{T}}}{\{ (f) \{ k_3^{\text{acid}} x_1 + k_3^{\text{base}} (1 - x_1) \} + (1 - f) k_2^{\text{acid}} x_1 \} [\text{buffer}]_{\text{T}}} \quad (7)$$

The intercept values obtained from the linear plots of  $1/k_{\text{obs}}$  vs  $1/[\text{buffer}]_{\text{T}}$  (Figure 3),  $Y$ , are found to depend linearly on  $1/[H^+]$  (Figure 5). From eq 7 results,

$$Y = \frac{([H^+] + K_a) \{ k_{-3}^{\text{acid}} x_1 + (k_{-3}^{\text{base}} + k_{-2}^{\text{base}})(1 - x_1) \} / k_6}{[H^+] \{ k_3^{\text{acid}} x_1 + k_3^{\text{base}} (1 - x_1) \} + K_a k_2^{\text{acid}} x_1} \quad (8)$$

where  $K_a = k_{-1}/k_1$ . Thus, and according to eq 8, a linear dependence on  $1/[H^+]$  requires the term  $(K_a k_2^{\text{acid}} x_1)$  in the denominator to be negligible. Microscopic reversibility requires that the term  $k_{-2}^{\text{base}}$  in the numerator of eq 8 to be negligible too. This is equivalent to say that the formation of *cis*-azonium ions takes place through the general acid/base-catalyzed pathway rather than through the pathway involving protonation at the azo group of *cis*-MO. For the latter mechanism, the degree of solvent reorganization involved is probably much larger than that for the former. Provided that these assumptions are valid, the ratio slope/intercept corresponding to plots of  $Y$  vs  $1/[H^+]$  would yield  $K_a$ , i.e., the acid dissociation equilibrium constant of *cis*-ammonium ions. For succinate and acetate buffers an average  $K_a$  value of  $1 \times 10^{-5}$  M is obtained. This value is significantly smaller than the reported acid dissociation equilibrium constant for

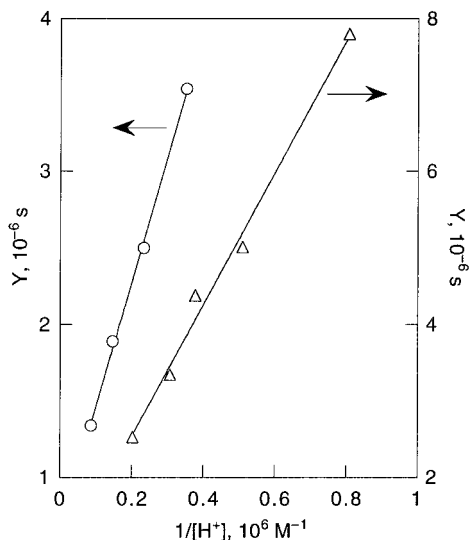
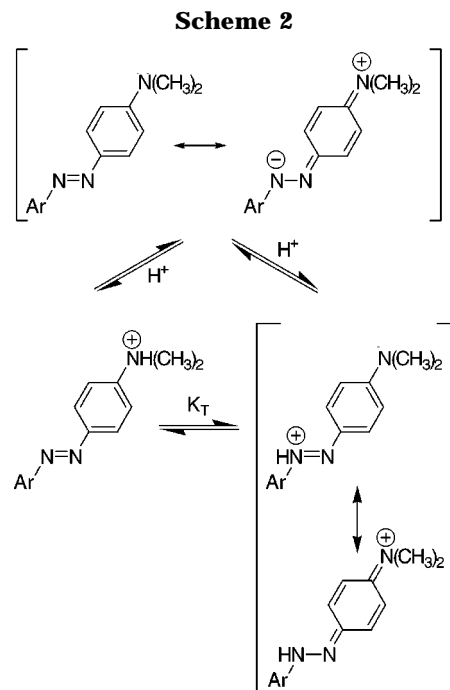


**Figure 5.** Plot of intercept values ( $Y$ , obtained from plots of  $1/k_{\text{obs}}$  vs  $1/[\text{buffer}]_T$ ) vs  $1/[\text{H}^+]$  corresponding to acetate buffer (O) and succinate buffer ( $\Delta$ ).

*trans*-ammonium ions (i.e.,  $\text{p}K_{\text{a}} = 2.70^{26}-2.87^{27}$ ). It should be pointed out here that the *trans* and *cis* forms of azobenzene and of some of its derivatives are known to have different basicities.<sup>17,28,29</sup> For instance, the  $\text{p}K_{\text{a}}$  values for *trans*- and *cis*-azobenzene are  $-2.95$  and  $-2.25$ , respectively,<sup>29</sup> whereas  $\text{p}K_{\text{a}}$  values of  $2.9$  and  $10.7$  were deduced for the *cis*-cation and *cis*-neutral species of 2-hydroxy-5-methylazobenzene, respectively, as compared to  $-1.5$  and  $9.4$  determined for the *trans* species.<sup>17</sup>

For *trans*-MO, as in the case of other 4-aminoazobenzenes, it has been shown that the  $\beta$ -nitrogen of the azo group ( $\text{p}K_{\text{a}} = 3.27^{26}-3.40^{27}$ ) is more basic than the amino nitrogen ( $\text{p}K_{\text{a}} = 2.70^{26}-2.87^{27}$ ). This result can be interpreted at least in part through resonance, which decreases the electron density at the amino nitrogen as well as increases the stability of the azonium species (Scheme 2). In the case of *cis*-MO, since the coplanarity between the azo group and the benzene rings is hindered for steric reasons, one could anticipate these resonance effects to be less effective. In fact, the *trans* form of azobenzene is known to be considerably more stable than the *cis* form, as a result of the resonance stabilization in the almost coplanar structure of the former. In *cis*-azobenzene the benzene rings are rotated out of the plane containing the azo group by ca.  $50^\circ$ , due to steric repulsion between the hydrogen atoms in the  $2,2'$ -positions.<sup>29</sup> Molecular modeling calculations, using the AM1 semiempirical method of HyperChem 3, allowed us to determine that in *cis*-MO the aryl rings containing the sulfonic and amino groups are rotated  $36^\circ$  and  $40^\circ$  out of the plane, respectively. Also, the resulting  $-\text{N}=\text{N}-$  bond lengths for *cis*-MO and *trans*-MO are  $1.20$  and  $1.23$  Å, respectively, consistent with a lower resonance interaction in the *cis* form. Thus, a greater basicity for the amino nitrogen (as well as a smaller tautomeric equilibrium constant,  $K_T$ ) in MO would be predicted for the *cis* isomer relative to the *trans*



form. In fact, the  $\text{p}K_{\text{a}}$  value of  $5$  determined from our experiments is quite similar to the  $\text{p}K_{\text{a}}$  value corresponding to *N,N*-dimethylanilinium ions (i.e.,  $\text{p}K_{\text{a}} = 5.15$ ).<sup>30</sup>

According to eq 8, and as a result of the linear dependence observed on  $1/[\text{H}^+]$ , eq 5 and 6 can be simplified to eq 9 and 10.

$$P(1) = (f)\{k_3^{\text{acid}}x_i + k_3^{\text{base}}(1 - x_i)\} \quad (9)$$

$$P(2) = \{k_{-3}^{\text{acid}}x_i + k_{-3}^{\text{base}}(1 - x_i)\}/k_6 \quad (10)$$

Analysis of the kinetic parameters  $P(1)/f$  (where  $f = \{[\text{H}^+]/([\text{H}^+] + 1 \times 10^{-5})\}$ ) and  $P(2)$  in terms of the molar fraction of the acidic component of the buffer ( $x_i$ ) yielded the catalytic coefficients given in Table 3. Using these values we could reproduce very well the experimental observed rate constants (relative error  $\leq 6\%$ ). Also, the ratios  $(k_3^{\text{acid}}k_6)/k_{-3}^{\text{acid}}$  and  $(k_3^{\text{base}}k_6)/k_{-3}^{\text{base}}$  are all about the same ( $1.2-1.4 \times 10^6 \text{ s}^{-1}$ ), with exception of the data for acetate which give a ratio somewhat higher ( $2.1 \times 10^6 \text{ s}^{-1}$ ) but still acceptable considering the propagation of errors. These ratios are expected to be all equal since they represent the product between the equilibrium constant for tautomerization ( $k_3/k_{-3}$ ) and the rate constant for isomerization ( $k_6$ ); this product should be independent of the type of acid and base employed. Comparison of the catalytic coefficients given in Table 3 clearly shows that the thermal *cis-trans* isomerization of MO is catalyzed by general acids and general bases. Interestingly, these observations are quite comparable to the catalysis observed in the case of the enolization of simple carbonyl compounds both by acids and bases.<sup>31</sup> The general acid-catalyzed and base-catalyzed tautomerization of MO are proposed to be represented as shown in Scheme 3, i.e., the transition states contain water, MO, and the general acid (AH) or base ( $\text{A}^-$ ). We noted that the participation

(26) Tawarah, K. M.; Abu-Shamleh, H. M. *Dyes Pigments* **1991**, *16*, 241.

(27) Reeves, R. L. *J. Am. Chem. Soc.* **1966**, *88*, 2240.

(28) Collins, J. H.; Jaffe, H. H. *J. Am. Chem. Soc.* **1962**, *84*, 4708.

(29) Krueger, P. J. *Basicity, hydrogen bonding and complex formation*; Krueger, P. J., Ed.; John Wiley and Sons: New York, 1975; Vol. 1, p 168.

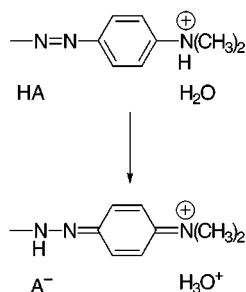
(30) *Handbook of Chemistry and Physics*; Lide, D. R., Ed.; CRC Press: Boca Raton, 1996-1997; pp 8-45.

(31) Hegarty, A. F.; Dowling, J. P.; Eustace, S. J.; McGarraghy, M. *J. Am. Chem. Soc.* **1998**, *120*, 2290.

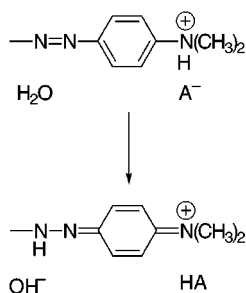
**Table 3.** Catalytic Constants for the Thermal *Cis-Trans* Isomerization of MO in Buffered Aqueous Solution<sup>a</sup>

acid	$pK_a^{a,b}$	$k_3^{\text{acid}}, 10^7 \text{ M}^{-1} \text{ s}^{-1}$	$k_3^{\text{base}}, 10^7 \text{ M}^{-1} \text{ s}^{-1}$	$k_{-3}^{\text{acid}}/k_6, \text{ M}^{-1}$	$k_{-3}^{\text{base}}/k_6, \text{ M}^{-1}$
CH <sub>3</sub> COOH	4.60	(18.9 ± 0.4)	(5.04 ± 0.09)	88 ± 13	44 ± 3
HOOCCH <sub>2</sub> COO <sup>-</sup>	5.20 <sup>c</sup>	(9.8 ± 0.2)	(9.8 ± 0.2)	80 ± 3	80 ± 3
H <sub>2</sub> PO <sub>4</sub> <sup>-</sup>	6.79	(3.2 ± 0.4)	(42.8 ± 0.7)	33 ± 11	303 ± 19

<sup>a</sup> At 21 °C,  $I = 0.2 \text{ M}$  (NaCl). <sup>b</sup> Determined potentiometrically. <sup>c</sup> In addition, a value of  $pK_{a1} = 3.90$  was determined.

**Scheme 3**  
General acid-catalyzed tautomerization

General base-catalyzed tautomerization



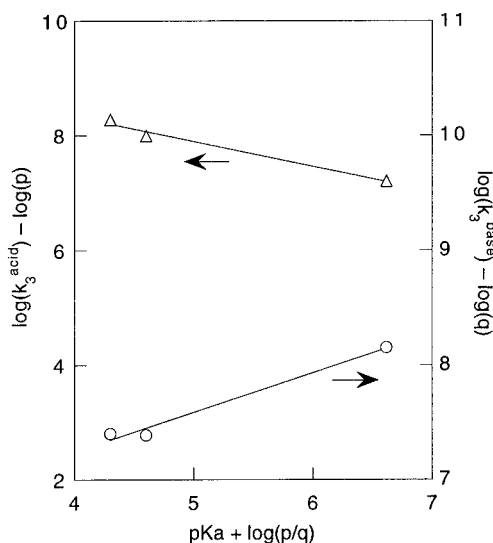
of two molecules of a protic solvent, one acting as a base and another as an acid, was previously proposed for the thermal isomerization of 1,3-diphenyltriazene.<sup>32</sup> Furthermore, the data in Table 3 shows that catalysis by general bases is characterized by a value of  $\beta = (0.33 \pm 0.07)$ , whereas catalysis by general acids has a value of  $\alpha = (0.38 \pm 0.07)$ . We are fully aware that these  $\alpha$  and  $\beta$  values are heavily influenced by the rate constants for phosphate buffer (Figure 6). Unfortunately the  $pK_a$  range cannot be expanded further: (i) at low pH the substrate precipitates, and (ii) at  $pH > 7$ , the reaction becomes too slow for our experimental technique.

In summary, as a result of an acid/base-assisted tautomerization of *cis*-ammonium ions into *cis*-azonium ions, the thermal *cis-trans* isomerization of MO is found to be catalyzed by general acids and general bases. *Cis*-azonium ions are proposed to easily isomerize via rotation around the  $-N=N-$  bond due to a decrease in the double bond character. Furthermore, *cis*-ammonium ions are estimated to be significantly less acidic than the isomeric *trans* ions, a result which is attributed to less effective resonance effects in the former due to steric reasons.

### Experimental Section

Methyl orange (Aldrich) was recrystallized from ethanol before use. Aqueous buffer solutions were prepared using reagent grade salts and water purified in a Millipore apparatus.

(32) Scaiano, J. C.; Chen, C.; McGarry, P. F. *J. Photochem. Photobiol., A: Chem.* **1991**, *62*, 75.

**Figure 6.** Brønsted plots for catalysis of the tautomerization of *cis*-MO by general acids ( $\Delta$ ) and general bases ( $\circ$ ).

Proton concentrations were calculated from the observed pH by using a value of 0.753 for the proton activity coefficient.<sup>33</sup> Molar fractions were calculated by using the acid dissociation equilibrium constants determined potentiometrically under our experimental conditions ( $\mu = 0.2 \text{ M}$ , 21 °C). Thus,  $pK_a$  values were obtained by extrapolating the pH values of solutions containing the acid and base forms in 1:1 ratio to zero concentration (Table 3); resulting values agree very well with those reported previously.<sup>34</sup>

Laser experiments were carried out using a Q-switched Nd:YAG laser (Continuum, Surelite I) operated at 355 nm (4–6 ns pulses, <30 mJ/pulse) for excitation. The system is controlled by a Power Mac 7100/80 computer running LabView 3.1.1 from National Instruments. This computer is interfaced (GPIB) to a Tektronix TDS 620 A digitizer used for data acquisition. Further details on this laser system have been reported elsewhere,<sup>35</sup> except that in the case of the experiments described in this work (i.e., transmission flash photolysis) a 150 W xenon lamp located behind the sample cell provided the monitoring beam, and the laser beam excited the sample at right angle to the monitoring beam. Solutions were contained in quartz cells constructed of  $7 \times 7 \text{ mm}^2$  Suprasil tubing. All measurements were performed at 21 °C.

**Acknowledgment.** This work was supported by research and equipment grants (to M.B.) from the Natural Sciences and Engineering Research Council of Canada. Special thanks are due to Mr. J. Szubra, Mr. D. Rieder, and Mr. I. Frola for technical assistance.

**Supporting Information Available:** Observed rate constants for thermal *cis-trans* isomerization of methyl orange in buffered aqueous solutions as a function of total buffer concentration and pH. This material is available free of charge via the Internet at <http://pubs.acs.org>.

JO982069J

(33) Harned, H. S.; Owen, B. B. *The physical chemistry of electrolytic solutions*; Reinhold Publishing Corporation: New York, 1958; p 748.

(34) Smith, R. M.; Martell, A. E. *Critical Stability Constants*; Plenum Press: New York, 1974; Vol. 6.

(35) Barra, M.; Agha, K. A. *J. Photochem. Photobiol. A: Chem.* **1997**, *109*, 293.